American Physiological Society | AMERICAN JOURNAL OF PHYSIOLOGY Endocrinology and Metabolism
PUBLISHED ARTICLE ARCHIVES SUBSCRIPTIONS SUBMISSIONS CONTACT US

Am J Physiol Endocrinol Metab. 2013 Jun 15; 304(12): E1303–E1313.
Published online 2013 Apr 9.
doi: 10.1152/ajpendo.00582.2012: 10.1152/ajpendo.00582.2012

PMCID: PMC3680696
PMID: 23571713

Excessive fructose intake causes 1,25-$(OH)_2D_3$-dependent inhibition of intestinal and renal calcium transport in growing rats

Veronique Douard,[1] Yves Sabbagh,[2] Jacklyn Lee,[1] Chirag Patel,[1] Francis W. Kemp,[3] John D. Bogden,[3] Sheldon Lin,[4] and Ronaldo P. Ferraris[1]

[1]Department of Pharmacology and Physiology, University of Medicine and Dentistry of New Jersey - New Jersey Medical School, Newark, New Jersey;
[2]Tissue Protection and Repair, Sanofi-Genzyme R&D Center, Genzyme, A Sanofi Company, Framingham, Massachusetts;
[3]Trace Element and Mineral Research Laboratory, Department of Preventive Medicine and Community Health, University of Medicine and Dentistry of New Jersey - New Jersey Medical School, Newark, New Jersey;
[4]Department of Orthopedics, University of Medicine and Dentistry of New Jersey - New Jersey Medical School, Newark, New Jersey
Corresponding author.
Address for reprint requests and other correspondence: R. P. Ferraris, Dept. of Pharmacology & Physiology, UMDNJ - New Jersey Medical School, 185 S. Orange Ave., MSB-H621, Newark, NJ 07101.

Received 2012 Nov 21; Accepted 2013 Apr 3.

Abstract

We recently discovered that chronic high fructose intake by lactating rats prevented adaptive increases in rates of active intestinal Ca^{2+} transport and in levels of 1,25-$(OH)_2D_3$, the active form of vitamin D. Since sufficient Ca^{2+} absorption is essential for skeletal growth, our discovery may explain findings that excessive consumption of sweeteners compromises bone integrity in children. We tested the hypothesis that 1,25-$(OH)_2D_3$ mediates the inhibitory effect of excessive fructose intake on active Ca^{2+} transport. First, compared with those fed glucose or starch, growing rats fed fructose for 4 wk had a marked reduction in intestinal Ca^{2+} transport rate as well as in expression of intestinal and renal Ca^{2+} transporters that was tightly associated with decreases in circulating levels of 1,25-$(OH)_2D_3$, bone length, and total bone ash weight but not with serum parathyroid hormone (PTH). Dietary fructose increased the expression of 24-hydroxylase (CYP24A1) and decreased that of 1α-hydroxylase (CYP27B1), suggesting that fructose might enhance the renal catabolism and impair the synthesis, respectively, of 1,25-$(OH)_2D_3$. Serum FGF23, which is secreted by osteocytes and inhibits CYP27B1 expression, was upregulated, suggesting a

potential role of bone in mediating the fructose effects on 1,25-$(OH)_2D_3$ synthesis. Second, 1,25-$(OH)_2D_3$ treatment rescued the fructose effect and normalized intestinal and renal Ca^{2+} transporter expression. The mechanism underlying the deleterious effect of excessive fructose intake on intestinal and renal Ca^{2+} transporters is a reduction in serum levels of 1,25-$(OH)_2D_3$. This finding is significant because of the large amounts of fructose now consumed by Americans increasingly vulnerable to Ca^{2+} and vitamin D deficiency.

Keywords: bone, growth, intestine, kidney, parathyroid hormone, vitamin D, FGF23

IN CHILDREN AND YOUNG ADULTS, excessive consumption of sugar-sweetened beverages and of sweets may increase the incidence of bone fracture, decrease bone mineral density (BMD), and reduce the rate of bone mineral accrual (35, 50). Moreover, chronic consumption of these sweeteners, including fructose, by young rats reduces bone mechanical strength and mineral content (11, 16, 48, 54) These studies suggest that sweeteners, including fructose, compromise bone integrity, but the mechanism remains unclear (49). Sufficient intake, intestinal absorption, and renal reabsorption of Ca^{2+} as well as increased levels of 1,25-$(OH)_2D_3$, or calcitriol, the active form of vitamin D_3, are essential in maintaining Ca^{2+} homeostasis and bone quality. Total intestinal Ca^{2+} absorption consists of a passive paracellular and a 1,25-$(OH)_2D_3$-dependent active transcellular pathway (21). Active Ca^{2+} transport involves Ca^{2+} entry through the apical transient receptor potential vanilloid Ca^{2+} channels (TRPV6 for the intestine and TRPV5 for the kidney), its intracellular diffusion via Ca^{2+}-binding proteins (CaBP9k for the intestine and CaBP28k for the kidney), and its extrusion across the intestinal or renal basolateral membrane through the Na^+/Ca^{2+} exchanger (NCX1) along with the plasma membrane Ca^{2+}-ATPase (PMCA1) (6). Since the major source for Ca^{2+} acquisition is intestinal absorption, vertebrates display adaptive increases in active Ca^{2+} transcellular transport, achieved by augmenting levels of 1,25-$(OH)_2D_3$, whenever physiological demands for Ca^{2+} increase. The precursor of vitamin D, cholecalciferol, is hydroxylated in the liver by 25-hydroxylases, producing calcidiol or 25-$(OH)D_3$, which is further hydroxylated in the kidney by 1α-hydroxylase (encoded by *CYP27B1*) to 1,25-$(OH)_2D_3$. Degradation of 25-$(OH)D_3$ and 1,25-$(OH)_2D_3$ is mediated by 24-hydroxylase (*CYP24A1*). Serum levels of 1,25-$(OH)_2D_3$ are tightly regulated by feedback loops controlling renal CYP27B1 and CYP24A1 expression (39).

We recently discovered in adult rat models of chronic kidney disease, as well as in lactating rats, that dietary fructose reduced rates of intestinal Ca^{2+} transport and circulating levels of 1,25-$(OH)_2D_3$, in association with a decrease in the binding of the vitamin D receptor (VDR) on the promoter of TRPV6 and CaBP9k genes (11, 16). This indicated that high fructose intake, by altering 1,25-$(OH)_2D_3$ homeostasis, may inhibit the adaptive increases in Ca^{2+} transport during lactation.

U.S. dietary intake data pooled by Popkin and Nielsen (40) show an 83 kcal/day increase of caloric sweetener consumption in the U.S. between 1962 and 2000. This upsurge represents a 22% increase in the proportion of daily energy requirements obtained from caloric sweeteners, including fructose. Fructose is transported passively across the apical membrane of the intestinal cell by the facilitative glucose transporter GLUT5 (*Slc2A5*), while the sodium-dependent glucose transporter SGLT1 (*Slc5A1*) is responsible for most glucose transport (14). Both sugars are then transported across the basolateral membrane by GLUT2 (*Slc2A2*) into the portal vein and the liver, where fructose is rapidly metabolized.

Many recent epidemiological studies correlate the rise in fructose consumption with various modern-day health concerns, including obesity, metabolic syndrome, and osteoporosis (5, 49). Since fructose is a natural component of human diets, its association with metabolic diseases may arise from recently documented, chronically excessive intake. Particular emphasis is placed on health concerns of actively growing children and adolescents whose intake per unit body weight of sweeteners, particularly fructose, is much greater than that of adults (34).

Few of the large number of studies on the metabolic effects of dietary fructose in humans and rodent models have utilized neonatal, weaning, or postweaning age groups (9, 10, 22, 25, 32), which consume the greatest quantity of fructose per kilogram of body weight. Since rapid growth in young mammals requires marked increases in Ca^{2+} intake and absorption driven by a higher level of 1,25-$(OH)_2D_3$ than older adults (17), we investigated in weaning rats the effect of a chronically high fructose intake on intestinal Ca^{2+} transport, 1,25-$(OH)_2D_3$ homeostasis, and bone quality. To test our hypothesis that the fructose-induced decrease in serum level of 1,25-$(OH)_2D_3$ is the mechanism by which dietary fructose impairs intestinal Ca^{2+} absorption, we then treated fructose-fed rats with 1,25-$(OH)_2D_3$ and determined whether the treatment prevented the deleterious effects of fructose.

MATERIALS AND METHODS

Animals. All the procedures in this study were approved by the Institutional Animal Care and Use Committee, UMDNJ-New Jersey Medical School. Studies were conducted on postweaning Sprague Dawley (Charles Rivers) male, virus/antibody-free rats (21 days old). Rats were kept under standard conditions: 12:12-h light-dark cycle and 22–24°C in dust-free cellulose bedding.

Experimental design. In the first study, postweaning rats (~55 g) were randomly divided into three groups (n = 7–9 rats) and then fed 63% glucose, fructose, or starch diets based on a standard American Institute of Nutrition (AIN)-93G formula containing normal Ca^{2+} and phosphate (Pi) levels designed to meet growth requirements of young rodents (11, 16). Animals were fed the diets ad libitum for 4 wk, from 21 to 50 days old. The AIN recommends either 73% (AIN-93M diet) or 63% (AIN-93G) carbohydrate levels, slightly higher than the average for humans (54%) consuming a high-carbohydrate diet (27). Since this is among the initial studies evaluating the effects of dietary fructose on 1,25-$(OH)_2D_3$ and Ca^{2+} homeostasis, we used an animal model with a high demand for these nutrients and then challenged this model with an experimental diet containing a high concentration of fructose to allow us to detect any potential effect it might have on selected outcomes. Although humans consume lower concentrations of fructose that are often mixed with other carbohydrates, studies have shown that mixing with glucose may accelerate fructose effects and that lower fructose concentrations cause similar deleterious effects to higher fructose concentrations if consumed for a longer time period (15, 24).

In a second study, same-age postweaning rats from a different batch (~45 g) were randomly divided into two groups fed a 63% glucose or fructose diet, and then each group was further subdivided into two subgroups (n = 6 rats), each receiving daily intraperitoneal injections at noon of either 2.4% (vol/vol) ethanol in saline (vehicle) or 1 μg/kg body wt 1,25-$(OH)_2D_3$ for 12 days. The animals were euthanized 18–20 h after the last 1,25-$(OH)_2D_3$ or saline injection.

In vitro intestinal nutrient transport measurements. Intestinal segments were everted quickly after isolation and prepared as everted sacs or sleeves to determine nutrient transport rates at 37°C with 95% O_2-5% CO_2 as described previously (11).

Ca^{2+} uptake. The everted gut sacs were made by using the first 4 cm of proximal duodenum, where active transcellular transport of Ca^{2+} is localized (4), and then incubated in Ca^{2+} transport buffer as previously described (11). The outer luminal and inner serosal compartments had equal initial concentrations (0.25 mM) of nonradioactive Ca^{2+}; then, $^{45}Ca^{2+}$ was added to the outer mucosal compartment. After 1 h, the active accumulation of $^{45}Ca^{2+}$ in the inner serosal compartment was calculated as a ratio of the final concentration of ($^{45}Ca^{2+}$ serosal/$^{45}Ca^{2+}$ mucosal compartments) and then normalized to that of rats fed starch.

Fructose and glucose uptake. Four 1-cm jejunal segments were made into everted sleeves, mounted on rods, and preincubated for 5 min in Krebs ringer bicarbonate (KRB) as described previously (12). Two segments each were then incubated in 50 mM glucose- or fructose-KRB solutions containing tracer concentrations of [^{14}C]glucose or [^{14}C]fructose, respectively.

Phosphate uptake. Intestinal Pi transport was determined in two consecutive 4-cm segments of medial jejunum using the previously described everted gut sac assay (11). Briefly, the everted intestinal segment for determining total Pi transport was incubated for 1 h in Na^+-containing Pi transport buffer (1.2 mM Pi), while the adjoining segment for determining Na^+-independent Pi transport was incubated in Na^+-free transport buffer. The total and Na^+-independent transport of ^{33}Pi was expressed as a ratio of the final concentration of (^{33}Pi serosal/^{33}Pi mucosal compartments) and normalized to the ratio obtained from sacs of rats fed starch.

Measurements of serum clinical parameters. Following earlier work (11), serum uric acid concentrations were determined using a QuantiChrom Uric Acid Assay Kit (BioAssay Systems, Hayward, CA), and Pi concentrations were determined using a QuantiChrom Pi Assay Kit. The total serum Ca^{2+} concentrations were determined by previously described techniques using flame atomic absorption spectrophotometry (model 603; PerkinElmer, Norwalk, CT) (11).

1,25-$(OH)_2D_3$, fibroblast growth factor 23, and PTH assays. Following earlier work (11, 53), serum 1,25-$(OH)_2D_3$ levels were measured by enzyme immunoassay [ImmunoDiagnosticSystems (IDS)]. Briefly, serum samples were delipidated and 1,25-$(OH)_2D_3$ immunoextracted before the assay. Serum 25-$(OH)D_3$ levels were measured directly by IDS. Intact rat PTH (Immutopics, San Clemente, CA) and intact fibroblast growth factor 23 (FGF23; Kainos, Tokyo, Japan) ELISAs were performed according to the manufacturers' instructions.

Real-time PCR. Total RNA from homogenized intestinal mucosa or kidney was isolated and reverse transcribed, and real-time PCR was performed using Mx3000P (Stratagene, La Jolla, CA) as previously described (13). The control group was the rats fed starch. The reference gene was α-elongation factor 1, *Ef1α*, whose expression is independent of age and dietary carbohydrate (12). Previously published primer sequences and annealing temperatures were used (11) (12).

Bone analyses. Briefly, harvested right femora were cleaned of soft tissues and stored at −20°C wrapped in saline-soaked gauze (0.9% NaCl) until testing. Prior to testing, the longitudinal length and the diameter at the diaphysis (the midsection of the shaft) were measured with a sliding caliper and recorded. The diameters were measured at the midshaft of the diaphysis. The maximum (a_o) and minimum (b_o) outer diameters were measured before breaking the bone, whereas the maximum (a_i) and minimum (b_i) inner diameters were measured after breaking. The cortical thickness was calculated by taking the difference between the maximum and minimum outer and inner diameters [max = $(a_o - a_i)/2$; min = $(b_o - b_i)/2$].

Determination of bone calcium, magnesium, and phosphorus. Harvested humera were dried to constant weight, and then organic materials in the dried bone were removed using a methanol-chloroform mixture (1:1 vol/vol). After extraction, bones were ashed overnight in a muffle furnace at 482°C. Ashed bones were dissolved in a hot nitric-perchloric acid mixture (3:1) and diluted to 25 ml with 1% nitric acid. For Ca^{2+} determinations, the samples were diluted with 0.05 M K-1% nitric acid. Then Ca^{2+} contents were determined by previously described techniques using flame atomic absorption spectrophotometry (Aanalyst 400; PerkinElmer Norwalk, CT) (47). For phosphorus, the samples were diluted in 12% trichloroacetic acid and iron molybdate solution to produce coloration within the range of standard concentrations prepared with KH_2PO_4 reagent. Samples are then read on a visible spectrum spectrophotometer at 660 nm.

Western blot analysis. Western blot analyses were performed using 50 μg of intestinal or renal protein extracts, following earlier work (11). Membranes were probed with polyclonal antibodies against CaBP9k (Swant Swiss Antibodies) and CYP27B1 (Santa Cruz Bioctechnologies) and then stripped and reprobed with β-actin antibody (Chemicon International).

Histology and immunohistochemistry. Immunohistochemistry was performed on kidney paraffin slides using rabbit anti-mouse NaPi2a [donated by Y. Sabbagh (42), 1:1,000 in 5% goat serum, in Pi-buffered saline (PBS)], incubated overnight at 4°C, and then washed in PBS. The secondary antibody was goat anti-rabbit IgG labeled with Cy3 (1:100, Chemicon International), diluted in 1% BSA in PBS, and applied for 1 h at 24°C. The stained sections were examined at ×20 or ×40 magnification with a laser scanning confocal microscope (Bio-Rad, Radiance 2100). All images of sections being compared were obtained with the same settings of the microscope. Nonspecific staining with secondary antibodies only was consistently negligible.

Statistical analyses. Data are presented as means ± SE. For the first experiment (4-wk feeding), a one-way ANOVA was used to determine the differences among groups with different diets. If there was a significant difference, Fisher's paired least significant difference (LSD) test was used (STATVIEW, Abacus Concepts) to determine differences among means. Differences were considered significant if $P < 0.05$. For the 1,25-$(OH)_2D_3$ rescue experiment, if an initial two-way ANOVA indicated a significant effect of 1,25-$(OH)_2D_3$ treatment and/or diet, a one-way ANOVA followed by LSD test was used to determine differences among means. Simple linear regressions were used to examine the relationship between circulating levels of 1,25-$(OH)_2D_3$ and FGF23 as well as between levels of 1,25-$(OH)_2D_3$ and PTH.

RESULTS

Fructose feeding inhibits Ca^{2+} transport. Chronic consumption of a high-fructose diet containing normal Ca^{2+} levels more than doubled intestinal fructose uptake but reduced active transepithelial Ca^{2+} transport by almost one-half compared with starch and glucose diets (Fig. 1*A*). The dietary fructose effect on Ca^{2+} and fructose transport is specific, because active glucose uptake, and total Pi transport, as well as Na^{+}-independent passive Pi transport, remained similar among the three diet groups.

To determine whether changes in transport rates paralleled changes in mRNA levels, we next analyzed expression of the various transporters that play significant roles in fructose and Ca^{2+} transport (Fig. 1*B*). mRNA levels of TRPV6 and CaBP9k each decreased more than threefold in the duodenum of fructose-fed rats, paralleling marked reductions in active Ca^{2+} transport. In contrast, the mRNA expression of GLUT5 was upregulated more than tenfold by dietary fructose. In the distal jejunum (data not shown), fructose also markedly downregulated TRPV6 and CaBP9k, except that mRNA expression levels were already orders of magnitude less than in the duodenum. These fructose effects on TRPV6, CaBP9k, and GLUT5 levels were specific, as expression of the basolateral Ca^{2+} transporters PMCA1 and NCX1 were not affected by the diet. Likewise, the mRNA expression of the Na^{+}/glucose cotransporter SGLT1 and the intestinal Na^{+}-dependent phosphate cotransporter NaPi2b remained independent of diet. Changes in protein levels of CaBP9k followed the changes observed for mRNA and showed a lower level of proteins in the intestine of fructose-fed rats (Fig. 1*C*).

Blood chemistry and hormone levels. We then investigated the plasma level of 1,25-$(OH)_2D_3$, since it is one of the key hormones controlling intestinal active Ca^{2+} transport, mainly by regulating TRPV6 and CaBP9k expression (Table 1). We observed a significant 30–40% decrease in 1,25-$(OH)_2D_3$ plasma concentration in rats fed fructose. It is well established that a low plasma level of Ca^{2+} promotes synthesis of PTH, which in turn increases 1,25-$(OH)_2D_3$ levels. Despite the marked decrease in rates of intestinal Ca^{2+} transport in the fructose group, plasma levels of Ca^{2+}, Pi, and PTH remained similar among the three diet groups. Since fructose may cause hyperuricemia arising from fructose-induced renal damage (37) and hepatic uric acid production (30), concentrations of uric acid were determined but were also found to be independent of diet.

Fructose alters CYP27B1 and CYP24A1 expression. We examined the effects of fructose on the kidney, since it is the major organ system regulating metabolism of 1,25-$(OH)_2D_3$, the hormone regulating intestinal Ca^{2+} transport. mRNA expression of *CYP27B1*, which synthesizes 1,25-$(OH)_2D_3$, was significantly downregulated threefold in the kidney of rats fed fructose compared with those fed glucose (Fig. 2*A*). In contrast, expression of *CYP24A1*, which catabolizes 1,25-$(OH)_2D_3$, was two- to threefold higher in fructose-fed than in both glucose- and starch-fed rats (Fig. 2*B*). The protein levels of CYP27B1 decreased in the kidney of fructose-fed rats (Fig. 2*C*). Thus, the decrease in circulating levels of 1,25-$(OH)_2D_3$ might have resulted from reduced synthesis and increased degradation.

We also performed gene expression analyses of 1,25-$(OH)_2D_3$ target genes in the kidney involved in Ca^{2+} reabsorption from glomerular filtrates (Fig. 2*D*). Expression levels of TRPV5 and CaBP28k decreased in the fructose-fed compared with the glucose- and starch-fed rats, an expression pattern similar to that observed for Ca^{2+}-transporting proteins in the small intestine. The mRNA expression of CaBP9k (the sole CaBP in the small intestine but also expressed in the kidney, where it serves a significant but supportive

role to CaBP28k), PMCA1 and NCX1 remained unchanged; thus, the inhibitory effect of fructose on TRPV5 and CaBP28k is specific. As in the small intestine, renal GLUT5 mRNA levels increased markedly, sixfold.

1,25-$(OH)_2D_3$ treatment rescues rats from the harmful effects of fructose. To prove that the deleterious effect of dietary fructose on intestinal Ca^{2+} transport was directly mediated by fructose-induced reductions in 1,25-$(OH)_2D_3$, fructose- and glucose (control)-fed rats were treated with 1,25-$(OH)_2D_3$. After 2 wk, fructose feeding caused a twofold decrease in duodenal Ca^{2+} transport in vehicle-treated rats (Fig. 3*A*). However, 1,25-$(OH)_2D_3$ treatment clearly prevented this deleterious effect of fructose. A similar, modest rescue effect of 1,25-$(OH)_2D_3$ was also observed on the mRNA expression level of TRPV6 and CaBP9k (Fig. 3*B*). In vehicle-treated rats, dietary fructose clearly reduced TRPV6 and CaBP9k mRNA expression more than twofold. This reduction was not observed in fructose-fed 1,25-$(OH)_2D_3$-treated rats. In glucose-fed rats, treatment with 1,25-$(OH)_2D_3$ did not induce any change in Ca^{2+} transport rate or in TRPV6 as well as CaBP9k mRNA expression but markedly increased the protein levels of CaBP9k (Fig. 3*C*). The protein level of CaBP9k also responded robustly to 1,25-$(OH)_2D_3$ treatment in fructose-fed rats.

Exogenous 1,25-$(OH)_2D_3$ also produced no toxic effects, since PMCA1, NCX1, and SGLT1 expression, which were not affected by diet, were also not affected by treatment with 1,25-$(OH)_2D_3$. In fact, 1,25-$(OH)_2D_3$ treatment did not interfere with regulation of vitamin D-independent genes, as clearly shown by the dramatic fructose-induced increase in GLUT5 expression in the presence or absence of 1,25-$(OH)_2D_3$.

What is the effect of exogenous 1,25-$(OH)_2D_3$ treatment on expression of CYP27B1 and CYP24A1? After 2 wk of feeding, the mRNA levels of CYP27B1 decreased threefold in fructose+vehicle rats (Fig. 4*A*). Treatment with exogenous 1,25-$(OH)_2D_3$ inhibited expression of renal CYP27B1 in both glucose- and fructose-fed rats, as would be expected since CYP27B1 is inhibited by its product (39). 1,25-$(OH)_2D_3$ treatment also decreased the protein levels of CYP27B1 in the glucose-fed rats (Fig. 4*C*). Since CYP27B1 protein levels were already very low in fructose-fed rats, 1,25-$(OH)_2D_3$ treatment resulted in no further decreases.

In contrast, 2 wk of dietary fructose was not sufficient to affect CYP24A1 expression (Fig. 4*B*). However, levels of CYP24A1 were already very low in this cohort of rats fed normal levels of Ca^{2+}, and further decreases would likely not have been detectable. Treatment with exogenous 1,25-$(OH)_2D_3$ stimulated expression of renal CYP24A1 in both glucose- and fructose-fed rats, as would be expected since CYP24A1 is stimulated by excess 1,25-$(OH)_2D_3$.

In the fructose+vehicle rats, serum 1,25-$(OH)_2D_3$ levels decreased by ~40% compared with those in the glucose+vehicle rats (Table 2), a trend similar to that observed in Table 1. It is not clear why there are differences in levels of hormones between experiments as indicated in Tables 1 and 2, but the second feeding experiment was conducted over a year after the first, so different batches of assay kits were used for analysis. Treatment with exogenous 1,25-$(OH)_2D_3$ further decreased serum 1,25-$(OH)_2D_3$, to 50% lower in both glucose- and fructose-fed rats compared with the glucose+vehicle group, for reasons mentioned in DISCUSSION. As expected, 1,25-$(OH)_2D_3$ treatment increased serum levels of Ca^{2+} in both glucose- and fructose-fed rats. Thus, as in the previous experiment, dietary fructose had no significant effect on Ca^{2+} levels.

The magnitude of the rescue effect of 1,25-$(OH)_2D_3$ was less marked in the kidney (Fig. 4*D*). TRPV5 expression decreased by over 50% in fructose+vehicle rats compared with that in glucose+vehicle rats. This inhibitory effect of fructose was clearly albeit modestly rescued by 1,25-$(OH)_2D_3$ treatment, as indicated by comparing the fructose+1,25-$(OH)_2D_3$ group to the glucose+vehicle and fructose+vehicle groups. 1,25-$(OH)_2D_3$ also hyperstimulated TRPV5 expression, as indicated by the ~50% increase in the glucose+1,25-$(OH)_2D_3$ rats. Fructose tended to reduce CaBP28k mRNA expression, and 1,25-$(OH)_2D_3$ treatment did not prevent this fructose-induced reduction in expression of CaBP28k in the kidney. Renal CaBP9k expression was similar between the glucose+vehicle and fructose+vehicle groups. Thus CaBP9k expression was not affected by dietary fructose, as was also observed in *experiment 1* (Fig. 2). Renal CaBP9k expression, however, was hyperstimulated by 1,25-$(OH)_2D_3$ treatment.

1,25-$(OH)_2D_3$ did not affect baseline PMCA1b and NCX1 expression. Moreover, 1,25-$(OH)_2D_3$ treatment did not interfere with regulation of GLUT5 expression, which increased markedly with dietary fructose in vehicle- and 1,25-$(OH)_2D_3$-injected rats. Thus, 1,25-$(OH)_2D_3$ treatment likely had no acute toxic effects on renal function, as in the small intestine.

Fructose increased FGF23 serum levels. Among the key regulators of 1,25-$(OH)_2D_3$ synthesis, FGF23 is known to reduce 1,25-$(OH)_2D_3$ levels by inhibiting CYP27B1 expression. We found that 4 wk of fructose feeding significantly increased circulating levels of FGF23 by more than 60% (Fig. 5*A*) and that there was a significant negative correlation between the serum levels of 1,25-$(OH)_2D_3$ and of FGF23 (Fig. 5*B*). PTH is another key factor regulating the circulating levels of 1,25-$(OH)_2D_3$. However, there was no significant correlation between the plasma levels of 1,25-$(OH)_2D_3$ and those of PTH (Fig. 5*C*), suggesting that the fructose-induced reduction in 1,25-$(OH)_2D_3$ levels may not involve PTH.

To support this new finding and demonstrate that fructose-induced increases in FGF23 affected the kidney, where 1,25-$(OH)_2D_3$ is synthesized, we investigated whether fructose feeding was associated with the well-established inhibitory effects of FGF23 on renal Pi reabsorption, as FGF23 inhibits the translocation of NaPi2a to the proximal tubular membranes (18, 42, 44). Fructose-fed rats (Fig. 6) clearly displayed a lower level of NaPi2a in the apical membrane of cells of the proximal tubules (white arrow) than those of rats fed glucose or starch.

Fructose feeding compromised growth rate. Despite similar rates of food intake among diets (data not shown) and similar rates of initial growth in the first week, rats fed fructose had slightly lower increases in body weight about 2 wk after the beginning of feeding compared with littermates fed glucose or starch (Fig. 7). After 2 wk more of feeding, at the time of death, the fructose group weighed ~7% less than the glucose or the starch group. This modest effect on body weight has been observed previously in other studies involving fructose feeding of postweaning rodents (25, 32).

The modest effect of fructose on body weight was also observed in *experiment 2*. Feeding rates and body weights were likewise similar at the start of the experiment when rats were 22 days of age, but at the midway point of the experiment after 7 days of feeding, fructose+vehicle rats exhibited a significantly ($P < 0.03$) lower body weight (67.6 ± 3.8 g) than glucose+vehicle rats (78.2 ± 2.5 g). Treatment with 1,25-$(OH)_2D_3$ prevented the fructose-induced, significant decrease in body weight (glucose-fed, 78.6 ± 2.8; fructose-fed, 73.2 ± 3.4 g; $P > 0.20$). At the end of the rescue experiment, ~12 days after initiation of feeding, fructose+vehicle rats (100 ± 5 g) had lower body weights than glucose+vehicle rats (124 ± 4 g).

However, the mean body weight of fructose+ 1,25-$(OH)_2D_3$ rats (110 ± 4 g) was not significantly different from that of glucose+1,25-$(OH)_2D_3$ rats (121 ± 4). Thus, 1,25-$(OH)_2D_3$ treatments partially rescued the rats from the deleterious effects of fructose on body weight.

Consequences of chronic fructose intake on bone. Fructose-fed rats had femur lengths significantly shorter than those of glucose- and starch-fed ones (Table 3), suggesting that the fructose-induced decrease in total body weight may have been due, in part, to retardation of linear skeletal growth. Although diet had no effect on outer bone diameters, glucose-fed rats tended to have greater inner bone diameters than fructose-fed and starch-fed rats. Thus, the net effect is a trend for glucose-fed rats to have less cortical thickness than fructose-fed and starch-fed rats.

Fructose-fed rats also displayed a lower (~10%) dry weight of the humeri than glucose and starch groups (Table 4). Subsequently, their bone ash weight was also significantly lower by ~12%; the percentage of bone ash to dry weight, however, was similar among the treatment groups. Bone Ca^{2+} was also higher in the glucose- and starch-fed rats, although the difference from that of the fructose-fed rats was not statistically significant. Glucose-fed rats contained a significantly higher amount of P than those fed fructose. The [Ca^{2+} × P] product accounts for much of the hydroxyapatite that makes up the bone matrix. [Ca^{2+} × P] tends to be lower in humeri of fructose-fed rats than in those fed glucose or starch, explaining their reduced length and lower weight.

DISCUSSION

The present study demonstrates that a decrease in circulating levels of 1,25-$(OH)_2D_3$ is the key mechanism by which fructose inhibits active transport of Ca^{2+} in the small intestine and likely in the kidney as well. This finding is highly significant, because total fructose intake now constitutes almost 10% of total energy intake of average Americans, and ~20% of total energy intake of the highest 5% of fructose consumers (34).

1,25-$(OH)_2D_3$ treatment prevents the fructose-induced decrease in intestinal Ca^{2+} transport. When Ca^{2+} status is deficient because dietary supply is limiting or physiological demand is high, levels of the biologically active 1,25-$(OH)_2D_3$ hormone increase dramatically to restore Ca^{2+} sufficiency by inducing active intestinal absorption and renal reabsorption of Ca^{2+}. We recently discovered that dietary fructose prevents these compensatory increases in Ca^{2+} transport in rats whose Ca^{2+} requirements are increased because of lactation (16). But the signal mediating the inhibitory fructose effect had not been clearly identified until the present study.

The fructose-induced decrease in intestinal Ca^{2+} transport was linked to reductions in duodenal expression of TRPV6 and CaBP9k, both known to be transcriptionally regulated by 1,25-$(OH)_2D_3$ (52). We focused on the duodenum because contributions of the more distal regions to adaptive, 1,25-$(OH)_2D_3$-mediated increases in active transcellular Ca^{2+} transport are likely to be small. Moreover, since fructose also decreases TRPV6 and CaBP9k expression levels in the distal jejunum, there likely can be no compensation of Ca^{2+} transport in these distal regions. CaBP9k-null mice are still able to transport Ca^{2+}; thus, CaBP9k deletion alone will not stop active transport (4). In TRPV6 knockout mice, Ca^{2+} absorption can still be stimulated by a low-Ca^{2+} diet and 1,25-$(OH)_2D_3$ injections (4, 28); hence, TRPV6 deletion alone is insufficient to fully inhibit transport activity. However, simultaneous deletion of TRPV6 and CaBP9k

impairs the ability to respond to Ca^{2+} insufficiency or 1,25-$(OH)_2D_3$ (4) treatment, indicating that both CaBP9k and TRPV6 are required for adaptive increases in Ca^{2+} transport. In our postweaning rat model requiring Ca^{2+} levels sufficient to support rapid growth, TRPV6 and CaBP9k expression was compromised by dietary fructose, providing a clue that 1,25-$(OH)_2D_3$ was involved.

Since serum levels of 1,25-$(OH)_2D_3$ decrease when it is injected (Table 2), how can 1,25-$(OH)_2D_3$ treatments rescue intestinal and renal Ca^{2+} transporters? The low serum 1,25-$(OH)_2D_3$ concentration is likely due to reductions in CYP27B1 expression and increases in CYP24A1 expression, potentially preventing the synthesis of endogenous 1,25-$(OH)_2D_3$ and ensuring the rapid clearance of injected 1,25-$(OH)_2D_3$. Similar findings had been previously observed in hypocalcemic CYP27B1-deficient mice treated daily with 1,25-$(OH)_2D_3$ for 5 wk that eventually rescued the hypocalcemia despite a dramatic increase in CYP24A1 expression and the undetectable amounts of 1,25-$(OH)_2D_3$ in the plasma (8).

Although 1,25-$(OH)_2D_3$ treatment clearly rescued intestinal Ca^{2+} transport, its acute effects on mRNA expression of intestinal target genes were modest. The acute effects of 1,25$(OH)_2D_3$ may be difficult to demonstrate due to the short half-life of intestinal CaBP9k [~16 h (2)] and TRPV6 [~6 h (46)] relative to the time gap between the last 1,25$(OH)_2D_3$ injection and death (~20 h). Thus, 1,25$(OH)_2D_3$-induced changes in levels of intestinal CaBP9k mRNA were small and contrasted with those of CaBP9k protein, which has a longer half-life and thus would be more reflective of acute 1,25$(OH)_2D_3$ effects. In vitamin D-deficient young rats, 1,25-$(OH)_2D_3$ treatment also caused gradual increases in CaBP9k mRNA and protein, but 24 h after injection, mRNA levels had returned to preinjection levels as protein levels remained high (2).

Although 1,25-$(OH)_2D_3$ treatment affects the paracellular component of Ca^{2+} transport, its effects are primarily on the active component, as indicated by the strikingly similar changes between active transepithelial transport and levels of intestinal TRPV6 and of CaBP9k expression (Figs. 1 and 3). Nonetheless, measurements of total and paracellular Ca^{2+} transport and of Ca^{2+} digestibility are very interesting and can be the subject of future work.

What is the mechanism underlying the fructose-induced decrease in 1,25-$(OH)_2D_3$? The proximate mechanism underlying the regulation of 1,25-$(OH)_2D_3$ by fructose may be the dramatic fructose-induced decreases in CYP27B1 expression and the increases in CYP24A1 expression as shown in the first experiment involving 5 wk of fructose feeding. In the second experiment, the renal expression of CYP27B1 was also reduced in fructose-fed compared with glucose-fed rats; however, the stimulatory fructose effect on CYP24A1 mRNA expression was not yet apparent, likely because fructose feeding lasted only 2 wk. When serum levels of Ca^{2+}, Pi, and 1,25-$(OH)_2D_3$ are normal, 1,25-$(OH)_2D_3$ inhibits its own synthesis by reducing CYP27B1 expression so that low levels of 1,25-$(OH)_2D_3$ are often associated with an increase in CYP27B1 expression to restore homeostasis. Since 1,25-$(OH)_2D_3$ levels and CYP27B1 expression are both low, the 1,25-$(OH)_2D_3$-CYP27B1 feedback loop is not responding appropriately in fructose-fed rats. This feedback loop was also shown by us to be disrupted in fructose-fed lactating rats (16), challenging our understanding of the regulation of 1,25-$(OH)_2D_3$ synthesis under conditions of chronically high fructose intake.

If this feedback loop is disrupted during chronic fructose feeding, what else may be mediating the fructose-induced reduction in 1,25-$(OH)_2D_3$? The two other main hormones potentially regulating 1,25-$(OH)_2D_3$ are PTH, which increases, and FGF23, which decreases, serum 1,25-$(OH)_2D_3$ concentrations (43). If the fructose-induced reduction in 1,25-$(OH)_2D_3$ concentrations is via PTH, fructose should reduce PTH levels; if via FGF23, fructose should increase FGF23 levels. In this study, PTH did not vary with diet, and there was no correlation between the circulating levels of PTH and 1,25-$(OH)_2D_3$, a finding similar to that in our previous work (16). In contrast, fructose increased FGF23 circulating levels, so that FGF23 and 1,25-$(OH)_2D_3$ were significantly negatively correlated. These findings suggest a potential role of FGF23 in the downregulation of 1,25-$(OH)_2D_3$ by fructose.

FGF23, which is highly expressed in bone tissue matrix-forming cells such as osteoblasts and osteocytes, is a phosphaturic hormone that decreases renal Pi reabsorption (43). We confirmed that the fructose-induced increase in FGF23 circulating levels is physiological, as it led to reduced translocation of NaPi2a protein expression to the apical membrane of proximal tubular cells, as previously shown (44). In fact, the marked effect of fructose via FGF23 on NaPi2a levels in the proximal tubular apical membrane (Fig. 6) may result in reduced Pi reabsorption as well as increased Pi excretion and may explain the increased loss of Pi from the bone (Table 4) to keep blood Pi levels from decreasing. In addition, FGF23 is known to regulate the renal synthesis of 1,25-$(OH)_2D_3$ by inhibiting CYP27B1 and stimulating CYP24A1 mRNA expression (43), findings replicated in this study. Future work using FGF23$^{-/-}$ and klotho$^{-/-}$ (the obligate renal coreceptor of FGF23) mice should confirm whether the effect of fructose is truly mediated through FGF23, and enable us to determine the mechanism underlying the fructose-induced increase in FGF23 concentrations.

It is not clear how fructose increases FGF23 levels, but 6-deoxy-6-[^{18}F]fluoro-D-fructose did accumulate in the bone more than in any other organ system (51). Interestingly, we have immunocytochemical evidence that GLUT5 may be expressed in bone (V. Douard and P. Ferraris, unpublished observations), suggesting that some bone cells may be able to transport and metabolize fructose. FGF23 is an early-onset biomarker of renal insufficiency (23), but it is also not clear whether this increase in FGF23 is a cause or a consequence of kidney damage (29, 41, 45). Interestingly, excessive fructose consumption has been shown to damage the kidney, as evidenced by marked renal hypertrophy, accelerated progression of chronic kidney disease, and apparent aggravation of end-stage renal disease symptoms (7, 11, 16, 19). It also increases plasma concentration of uric acid (31), shown to be positively associated with increased FGF23 in adults and children with normal kidney function (3, 20). However, in this study, the rats fed fructose did not yet exhibit any increase in plasma levels of uric acid, although fructose did induce renal hypertrophy.

A recent study showed that FGF23 may directly alter 1,25-$(OH)_2D_3$-mediated intestinal Ca^{2+} transport in mice (26), suggesting that FGF23 may not act indirectly via the kidney. However, klotho is an obligate coreceptor of FGF receptors for FGF23 that is expressed at high levels only in the kidney and is poorly expressed in the small intestine (38); thus, it is not clear how FGF23 would exert its direct effects on the gut.

Fructose and growth. Although serum Ca^{2+} concentrations were not perturbed, preserving its essential electrochemical gradients and cell signaling functions, fructose-induced reductions in Ca^{2+} transport may ultimately have affected growth rate, as indicated by reductions in bone length, bone dry weight, and body

weight. The cause can only be ascribed to excessive fructose intake, as the diets were isocaloric and isonitrogenous. The effect of chronic fructose feeding on body weight observed in both experiments may be specific for this rapidly growing age group, as we did not observe such fructose effects on body weight in our previous studies involving adult male and female rats (11, 16). Two other studies focusing on fructose effects in postweaning rats also observed reductions in body weight (25, 32) between 4 and 8 wk of age. Continued fructose feeding in one study beyond 8 wk of age eventually led to the frequently observed fructose-induced increases in body weight and obesity in older age groups.

Modest differences in food intake were observed only after body weight was reduced, and even then, food consumption per kilogram of body weight remained the same. Thus, both Ca^{2+} and 1,25-$(OH)_2D_3$ are critical for bone development, and herein we confirm, using a fructose model, previous work demonstrating that the action of 1,25-$(OH)_2D_3$ on the contributions of Ca^{2+} to bone growth and remodeling is mediated by regulating intestinal Ca^{2+} absorption (1, 33). In contrast, fructose seems to influence Pi levels and metabolism in bone without affecting total and Na^+-independent Pi transport in the small intestine. However, fructose, via an increase in serum FGF23 level, decreased expression of NaPi2a in the apical membrane of the proximal tubule, which likely impaired renal reabsorption of Pi. Interestingly, consumption by humans of a high-fructose diet (20% of total calories) for 5 wk markedly increased renal Pi excretion, modestly increased renal Ca^{2+} excretion, and compromised intestinal Ca^{2+} absorption, thereby decreasing Ca^{2+} and Pi balance (36). Our findings provide a mechanism underlying these interesting observations.

Perspectives. In conclusion, our studies demonstrate that a chronically high fructose intake during postweaning has adverse impacts on the intestine, kidney, and bone (Fig. 8). More studies are required in order to better understand the exact signaling pathways involved in the different organs impacted by excess fructose intake and to demonstrate that a mixed diet with lower fructose content will have similar effects as was demonstrated previously (15, 24). Here, we used the same high fructose concentration as in an earlier work (16) to demonstrate that our previous observation in the rat lactation model could be repeated in growing rats that were not hyperphagic, to demonstrate a robust effect of fructose so that we could unequivocally show whether or not 1,25-$(OH)_2D_3$ mediated those effects, and to induce the fructose effect quickly and demonstrate 1,25-$(OH)_2D_3$ mediation while growth rate was still rapid.

GRANTS

This work was supported in part by NSF Grants IOS-1121049; and 0722365. Support from National Institutes of Health Grant RC1-AI-078518, Foundation of UMDNJ, and Benjamin Delessert Foundation (to V. Douard) are also acknowledged.

DISCLOSURES

No conflicts of interest, financial or otherwise, are declared by the author(s).

AUTHOR CONTRIBUTIONS

Author contributions: V.D. and R.P.F. conception and design of research; V.D., Y.S., J.L., C.P., and F.W.K. performed experiments; V.D., Y.S., J.L., C.P., F.W.K., J.D.B., S.L., and R.P.F. analyzed data; V.D., Y.S., C.P., J.D.B., S.L., and R.P.F. interpreted results of experiments; V.D., J.L., and R.P.F. prepared figures; V.D. drafted manuscript; V.D., Y.S., J.D.B., and R.P.F. edited and revised manuscript; R.P.F. approved final version of manuscript.

ACKNOWLEDGMENTS

We are grateful to Dr. David Paglia for technical advice, Dr. Peddrick Weis for the use of the muffle furnace and laboratory, and Humberto Cruz, Ashkan Hamzelou, and Frank Portugal for technical help.

REFERENCES

1. Amling M, Priemel M, Holzmann T, Chapin K, Rueger JM, Baron R, Demay MB. Rescue of the skeletal phenotype of Vitamin D receptor-ablated mice in the setting of normal mineral ion homeostasis: formal histomorphometric and biomechanical analyses. Endocrinology 140: 4982–4987, 1999 [PubMed: 10537122]

2. Armbrecht HJ, Boltz MA, Christakos S, Bruns ME. Capacity of 1,25-dihydroxyvitamin D to stimulate expression of calbindin D changes with age in the rat. Arch Biochem Biophys 352: 159–164, 1998 [PubMed: 9587402]

3. Bacchetta J, Cochat P, Salusky IB, Wesseling-Perry K. Uric acid and IGF1 as possible determinants of FGF23 metabolism in children with normal renal function. Pediatr Nephrol 27: 1131–1138, 2012 [PMCID: PMC3793329] [PubMed: 22311343]

4. Benn BS, Ajibade D, Porta A, Dhawan P, Hediger M, Peng JB, Jiang Y, Oh GT, Jeung EB, Lieben L, Bouillon R, Carmeliet G, Christakos S. Active intestinal calcium transport in the absence of transient receptor potential vanilloid type 6 and calbindin-D9k. Endocrinology 149: 3196–3205, 2008 [PMCID: PMC2408805] [PubMed: 18325990]

5. Bray GA, Nielsen SJ, Popkin BM. Consumption of high-fructose corn syrup in beverages may play a role in the epidemic of obesity. Am J Clin Nutr 79: 537–543, 2004 [PubMed: 15051594]

6. Christakos S. Recent advances in our understanding of 1,25-dihydroxyvitamin D(3) regulation of intestinal calcium absorption. Arch Biochem Biophys 523: 73–76, 2012 [PMCID: PMC3339283] [PubMed: 22230327]

7. Cirillo P, Gersch MS, Mu W, Scherer PM, Kim KM, Gesualdo L, Henderson GN, Johnson RJ, Sautin YY. Ketohexokinase-dependent metabolism of fructose induces proinflammatory mediators in proximal tubular cells. J Am Soc Nephrol 20: 545–553, 2009 [PMCID: PMC2653686] [PubMed: 19158351]

8. Dardenne O, Prudhomme J, Hacking SA, Glorieux FH, St-Arnaud R. Rescue of the pseudo-vitamin D deficiency rickets phenotype of CYP27B1-deficient mice by treatment with 1,25-dihydroxyvitamin D3: biochemical, histomorphometric, and biomechanical analyses. J Bone Miner Res 18: 637–643, 2003 [PubMed: 12674324]

9. David ES, Cingari DS, Ferraris RP. Dietary induction of intestinal fructose absorption in weaning rats. Pediatr Res 37: 777–782, 1995 [PubMed: 7651763]

10. de Moura RF, Ribeiro C, de Oliveira JA, Stevanato E, de Mello MA. Metabolic syndrome signs in Wistar rats submitted to different high-fructose ingestion protocols. Br J Nutr 101: 1178–1184, 2009 [PubMed: 19007450]

11. Douard V, Asgerally A, Sabbagh Y, Sugiura S, Shapses SA, Casirola D, Ferraris RP. Dietary fructose inhibits intestinal calcium absorption and induces vitamin D insufficiency in CKD. J Am Soc Nephrol 21: 261–271, 2010 [PMCID: PMC2834550] [PubMed: 19959720]

12. Douard V, Choi HI, Elshenawy S, Lagunoff D, Ferraris RP. Developmental reprogramming of rat GLUT5 requires glucocorticoid receptor translocation to the nucleus. J Physiol 586: 3657–3673, 2008 [PMCID: PMC2538831] [PubMed: 18556366]

13. Douard V, Cui XL, Soteropoulos P, Ferraris RP. Dexamethasone sensitizes the neonatal intestine to fructose induction of intestinal fructose transporter (Slc2A5) function. Endocrinology 149: 409–423, 2008 [PMCID: PMC2194616] [PubMed: 17947353]

14. Douard V, Ferraris RP. Regulation of the fructose transporter GLUT5 in health and disease. Am J Physiol Endocrinol Metab 295: E227–E237, 2008 [PMCID: PMC2652499] [PubMed: 18398011]

15. Douard V, Sabbagh Y, Suzuki T, Ferraris R. A high fructose intake prevents compensatory increases in intestinal calcium transport in rodent models physiologically and nutritionally deficient in calcium. Digestive Disease Week, San Diego. Gastroenterology, 2012, p. S557

16. Douard V, Suzuki T, Sabbagh Y, Lee J, Shapses S, Lin S, Ferraris RP. Dietary fructose inhibits lactation-induced adaptations in rat 1,25-(OH)(2)D(3) synthesis and calcium transport. FASEB J 26: 707–721, 2012 [PMCID: PMC3290445] [PubMed: 22038050]

17. Fujisawa Y, Kida K, Matsuda H. Role of change in vitamin D metabolism with age in calcium and phosphorus metabolism in normal human subjects. J Clin Endocrinol Metab 59: 719–726, 1984 [PubMed: 6541227]

18. Gattineni J, Bates C, Twombley K, Dwarakanath V, Robinson ML, Goetz R, Mohammadi M, Baum M. FGF23 decreases renal NaPi-2a and NaPi-2c expression and induces hypophosphatemia in vivo predominantly via FGF receptor 1. Am J Physiol Renal Physiol 297: F282–F291, 2009 [PMCID: PMC2724258] [PubMed: 19515808]

19. Gersch MS, Mu W, Cirillo P, Reungjui S, Zhang L, Roncal C, Sautin YY, Johnson RJ, Nakagawa T. Fructose, but not dextrose, accelerates the progression of chronic kidney disease. Am J Physiol Renal Physiol 293: F1256–F1261, 2007 [PubMed: 17670904]

20. Gutierrez OM, Wolf M, Taylor EN. Fibroblast growth factor 23, cardiovascular disease risk factors, and phosphorus intake in the health professionals follow-up study. Clin J Am Soc Nephrol 6: 2871–2878, 2011 [PMCID: PMC3255372] [PubMed: 22034506]

21. Hoenderop JGJ, Nilius B, Bindels RJM. Calcium absorption across epithelia. Physiol Rev 85: 373–422, 2005 [PubMed: 15618484]

22. Huynh M, Luiken JJ, Coumans W, Bell RC. Dietary fructose during the suckling period increases body weight and fatty acid uptake into skeletal muscle in adult rats. Obesity (Silver Spring) 16: 1755–1762, 2008 [PubMed: 18483476]

23. Isakova T, Wahl P, Vargas GS, Gutierrez OM, Scialla J, Xie H, Appleby D, Nessel L, Bellovich K, Chen J, Hamm L, Gadegbeku C, Horwitz E, Townsend RR, Anderson CA, Lash JP, Hsu CY, Leonard MB, Wolf M. Fibroblast growth factor 23 is elevated before parathyroid hormone and phosphate in chronic kidney disease. Kidney Int 79: 1370–1378, 2011 [PMCID: PMC3134393] [PubMed: 21389978]

24. Johnson RJ, Perez-Pozo SE, Sautin YY, Manitius J, Sanchez-Lozada LG, Feig DI, Shafiu M, Segal M, Glassock RJ, Shimada M, Roncal C, Nakagawa T. Hypothesis: could excessive fructose intake and uric acid cause type 2 diabetes? Endocr Rev 30: 96–116, 2009 [PMCID: PMC2647706] [PubMed: 19151107]

25. Kawasaki T, Kashiwabara A, Sakai T, Igarashi K, Ogata N, Watanabe H, Ichiyanagi K, Yamanouchi T. Long-term sucrose-drinking causes increased body weight and glucose intolerance in normal male rats. Br J Nutr 93: 613–618, 2005 [PubMed: 15975159]

26. Khuituan P, Teerapornpuntakit J, Wongdee K, Suntornsaratoon P, Konthapakdee N, Sangsaksri J, Sripong C, Krishnamra N, Charoenphandhu N. Fibroblast growth factor-23 abolishes 1,25-dihydroxyvitamin D_3-enhanced duodenal calcium transport in male mice. Am J Physiol Endocrinol Metab 302: E903–E913, 2012 [PubMed: 22275752]

27. Krauss RM, Blanche PJ, Rawlings RS, Fernstrom HS, Williams PT. Separate effects of reduced carbohydrate intake and weight loss on atherogenic dyslipidemia. Am J Clin Nutr 83: 1025–1031; quiz 1205, 2006 [PubMed: 16685042]

28. Kutuzova GD, Sundersingh F, Vaughan J, Tadi BP, Ansay SE, Christakos S, Deluca HF. TRPV6 is not required for 1alpha,25-dihydroxyvitamin D3-induced intestinal calcium absorption in vivo. Proc Natl Acad Sci USA 105: 19655–19659, 2008 [PMCID: PMC2605002] [PubMed: 19073913]

29. Lafage-Proust MH. Does the downregulation of the FGF23 signaling pathway in hyperplastic parathyroid glands contribute to refractory secondary hyperparathyroidism in CKD patients? Kidney Int 77: 390–392, 2010 [PubMed: 20150940]

30. Lanaspa MA, Sanchez-Lozada LG, Choi YJ, Cicerchi C, Kanbay M, Roncal-Jimenez CA, Ishimoto T, Li N, Marek G, Duranay M, Schreiner G, Rodriguez-Iturbe B, Nakagawa T, Kang DH, Sautin YY, Johnson RJ. Uric acid induces hepatic steatosis by generation of mitochondrial oxidative stress: potential role in fructose-dependent and-independent fatty liver. J Biol Chem 287: 40732–40744, 2012 [PMCID: PMC3504786] [PubMed: 23035112]

31. Le KA, Tappy L. Metabolic effects of fructose. Curr Opin Clin Nutr Metab Care 9: 469–475, 2006 [PubMed: 16778579]

32. Lewis CG, Fields M, Beal T. The effect of various levels of fructose in a copper-deficient diet on Cu deficiency in male rats. Br J Nutr 63: 387–395, 1990 [PubMed: 2334672]

33. Lieben L, Masuyama R, Torrekens S, Van Looveren R, Schrooten J, Baatsen P, Lafage-Proust MH, Dresselaers T, Feng JQ, Bonewald LF, Meyer MB, Pike JW, Bouillon R, Carmeliet G. Normocalcemia is maintained in mice under conditions of calcium malabsorption by vitamin D-induced inhibition of bone mineralization. J Clin Invest 122: 1803–1815, 2012 [PMCID: PMC3336970] [PubMed: 22523068]

34. Marriott BP, Cole N, Lee E. National estimates of dietary fructose intake increased from 1977 to 2004 in the United States. J Nutr 139: 1228S–1235S, 2009 [PubMed: 19403716]

35. McGartland C, Robson PJ, Murray L, Cran G, Savage MJ, Watkins D, Rooney M, Boreham C. Carbonated soft drink consumption and bone mineral density in adolescence: the Northern Ireland Young Hearts Project. J Bone Miner Res 18: 1563–1569, 2003 [PubMed: 12968664]

36. Milne DB, Nielsen FH. The interaction between dietary fructose and magnesium adversely affects macromineral homeostasis in men. J Am Coll Nutr 19: 31–37, 2000 [PubMed: 10682873]

37. Nakagawa T, Hu H, Zharikov S, Tuttle KR, Short RA, Glushakova O, Ouyang X, Feig DI, Block ER, Herrera-Acosta J, Patel JM, Johnson RJ. A causal role for uric acid in fructose-induced metabolic syndrome. Am J Physiol Renal Physiol 290: F625–F631, 2006 [PubMed: 16234313]

38. Ohyama Y, Kurabayashi M, Masuda H, Nakamura T, Aihara Y, Kaname T, Suga T, Arai M, Aizawa H, Matsumura Y, Kuro-o M, Nabeshima Y, Nagail R. Molecular cloning of rat klotho cDNA: markedly decreased expression of klotho by acute inflammatory stress. Biochem Biophys Res Commun 251: 920–925, 1998 [PubMed: 9791011]

39. Omdahl JL, Morris HA, May BK. Hydroxylase enzymes of the vitamin D pathway: expression, function, and regulation. Annu Rev Nutr 22: 139–166, 2002 [PubMed: 12055341]

40. Popkin BM, Nielsen SJ. The sweetening of the world's diet. Obes Res 11: 1325–1332, 2003 [PubMed: 14627752]

41. Razzaque MS. The FGF23-Klotho axis: endocrine regulation of phosphate homeostasis. Nat Rev Endocrinol 5: 611–619, 2009 [PMCID: PMC3107967] [PubMed: 19844248]

42. Sabbagh Y, O'Brien SP, Song W, Boulanger JH, Stockmann A, Arbeeny C, Schiavi SC. Intestinal npt2b plays a major role in phosphate absorption and homeostasis. J Am Soc Nephrol 20: 2348–2358, 2009 [PMCID: PMC2799172] [PubMed: 19729436]

43. Shimada T, Hasegawa H, Yamazaki Y, Muto T, Hino R, Takeuchi Y, Fujita T, Nakahara K, Fukumoto S, Yamashita T. FGF-23 is a potent regulator of vitamin D metabolism and phosphate homeostasis. J Bone Miner Res 19: 429–435, 2004 [PubMed: 15040831]

44. Shimada T, Kakitani M, Yamazaki Y, Hasegawa H, Takeuchi Y, Fujita T, Fukumoto S, Tomizuka K, Yamashita T. Targeted ablation of Fgf23 demonstrates an essential physiological role of FGF23 in phosphate and vitamin D metabolism. J Clin Invest 113: 561–568, 2004 [PMCID: PMC338262] [PubMed: 14966565]

45. Shimada T, Urakawa I, Isakova T, Yamazaki Y, Epstein M, Wesseling-Perry K, Wolf M, Salusky IB, Juppner H. Circulating fibroblast growth factor 23 in patients with end-stage renal disease treated by peritoneal dialysis is intact and biologically active. J Clin Endocrinol Metab 95: 578–585, 2010

[PMCID: PMC2840849] [PubMed: 19965919]

46. Song Y, Fleet JC. Intestinal resistance to 1,25 dihydroxyvitamin D in mice heterozygous for the vitamin D receptor knockout allele. Endocrinology 148: 1396–1402, 2007 [PMCID: PMC2617756] [PubMed: 17110426]

47. Sugiura SH, Kelsey K, Ferraris RP. Molecular and conventional responses of large rainbow trout to dietary phosphorus restriction. J Comp Physiol B 177: 461–472, 2007 [PubMed: 17279387]

48. Tjaderhane L, Larmas M. A high sucrose diet decreases the mechanical strength of bones in growing rats. J Nutr 128: 1807–1810, 1998 [PubMed: 9772153]

49. Tsanzi E, Fitch CW, Tou JC. Effect of consuming different caloric sweeteners on bone health and possible mechanisms. Nutr Rev 66: 301–309, 2008 [PubMed: 18522618]

50. Tucker KL, Morita K, Qiao N, Hannan MT, Cupples LA, Kiel DP. Colas, but not other carbonated beverages, are associated with low bone mineral density in older women: The Framingham Osteoporosis Study. Am J Clin Nutr 84: 936–942, 2006 [PubMed: 17023723]

51. Wuest M, Trayner BJ, Grant TN, Jans HS, Mercer JR, Murray D, West FG, McEwan AJ, Wuest F, Cheeseman CI. Radiopharmacological evaluation of 6-deoxy-6-[18F]fluoro-d-fructose as a radiotracer for PET imaging of GLUT5 in breast cancer. Nucl Med Biol 38: 461–475, 2011 [PubMed: 21531283]

52. Xue Y, Fleet JC. Intestinal vitamin D receptor is required for normal calcium and bone metabolism in mice. Gastroenterology 136: 1317–1327, e1311–e1312, 2009 [PMCID: PMC2695717] [PubMed: 19254681]

53. Yu X, Sabbagh Y, Davis SI, Demay MB, White KE. Genetic dissection of phosphate- and vitamin D-mediated regulation of circulating Fgf23 concentrations. Bone 36: 971–977, 2005 [PubMed: 15869926]

54. Zernicke RF, Salem GJ, Barnard RJ, Schramm E. Long-term, high-fat-sucrose diet alters rat femoral neck and vertebral morphology, bone mineral content, and mechanical properties. Bone 16: 25–31, 1995 [PubMed: 7742079]

Figures and Tables

Fig. 1.

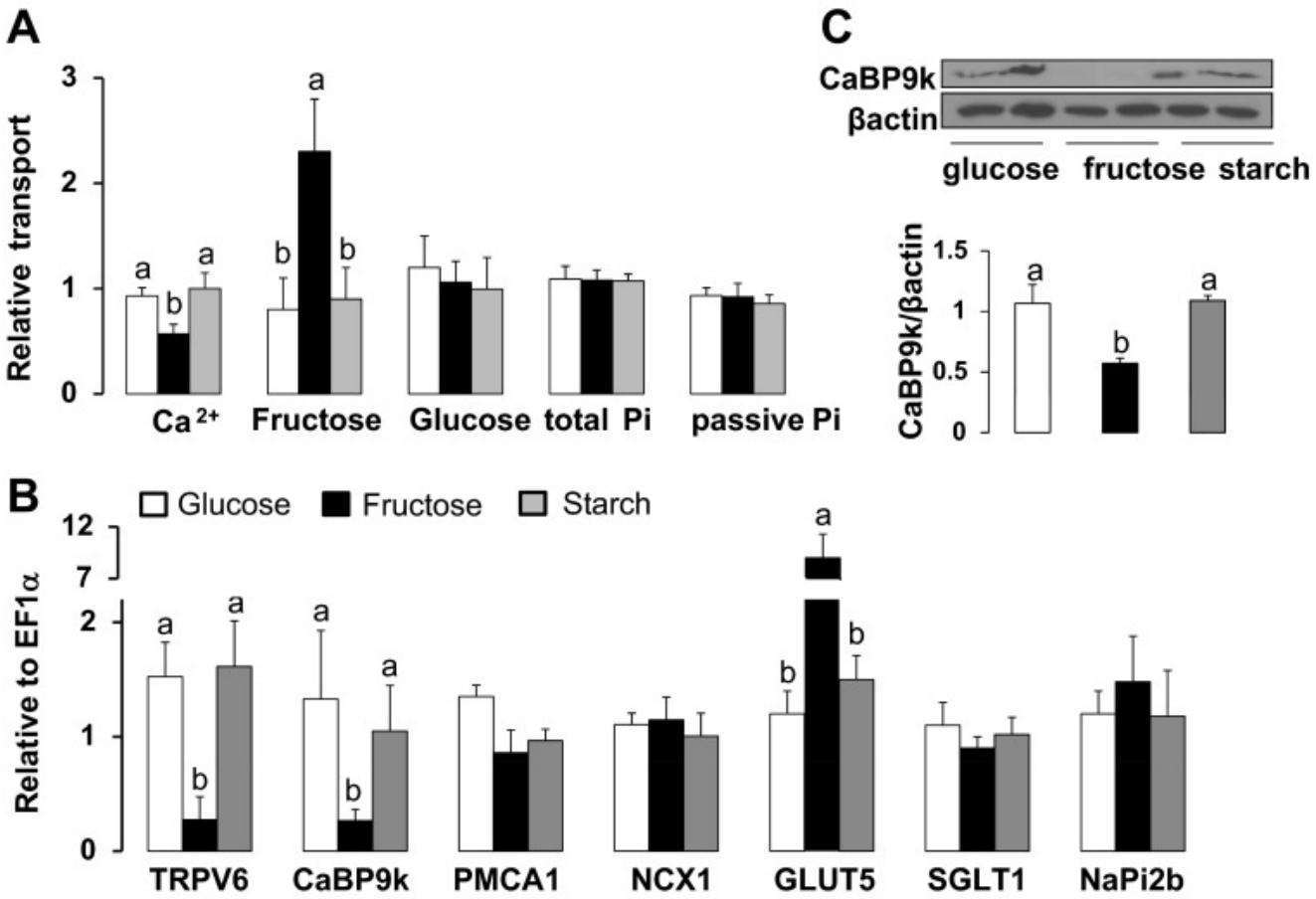

Open in a separate window

Intestinal Ca^{2+}, fructose, glucose, and Pi transport and transporter expression in 50-day-old rat fed glucose, fructose, or starch after weaning. *A*: Ca^{2+} and Pi transport were measured using everted intestinal sacs formed from the duodenum and proximal jejunum, respectively. Relative transepithelial Ca^{2+} and Pi transport from the luminal to the basolateral compartment were expressed as a ratio of ($^{45}Ca^{2+}_{inside}/^{45}Ca^{2+}_{outside}$ or $^{33}Pi_{inside}/^{33}Pi_{outside}$, respectively) of the everted sacs. Relative fructose and glucose uptakes into enterocytes were measured using everted intestinal sleeves from the jejunum. *B*: mRNA expression of Ca^{2+} (TRPV6, CaBP9k, PMCA1, NCX1) fructose (GLUT5), glucose (SGLT1), and phosphate (NaPi2b) transporters was analyzed by real-time PCR using *EF1α* as a reference. All data were normalized relative to levels seen in rat fed starch. Data are means ± SE ($n = 8$ per group). Means with different superscript letters are significantly different at $P < 0.05$. *C*: protein abundance of CaBP9k using β-actin as a reference. Ca^{2+} transport and transporter expression decreased with chronic consumption of fructose.

Table 1.

Serum biochemistry in 50-day-old rats fed glucose, fructose, or starch diet for 4 wk

	Glucose	Fructose	Starch	Significance
1,25-$(OH)_2D_3$, pmol/l	949 ± 28[a]	638 ± 50[b]	885 ± 22[a]	<0.001
PTH, pg/ml	257 ± 62	200 ± 25	164 ± 32	0.568
Calcium, mg/dl	11.5 ± 0.3	10.2 ± 0.8	11.5 ± 0.2	0.165
Phosphate, mg/dl	18.9 ± 1.4	17.7 ± 1.1	18.5 ± 1.4	0.679
Uric acid, mg/dl	3.8 ± 0.19	3.5 ± 0.04	3.2 ± 0.23	0.124

Data are means ± SE; n = 7–9 per group. Superscript letters refer to results of least significant difference (LSD) post hoc tests after one-way ANOVA ($P < 0.05$). Means with different superscript letters are significantly different.

Fig. 2.

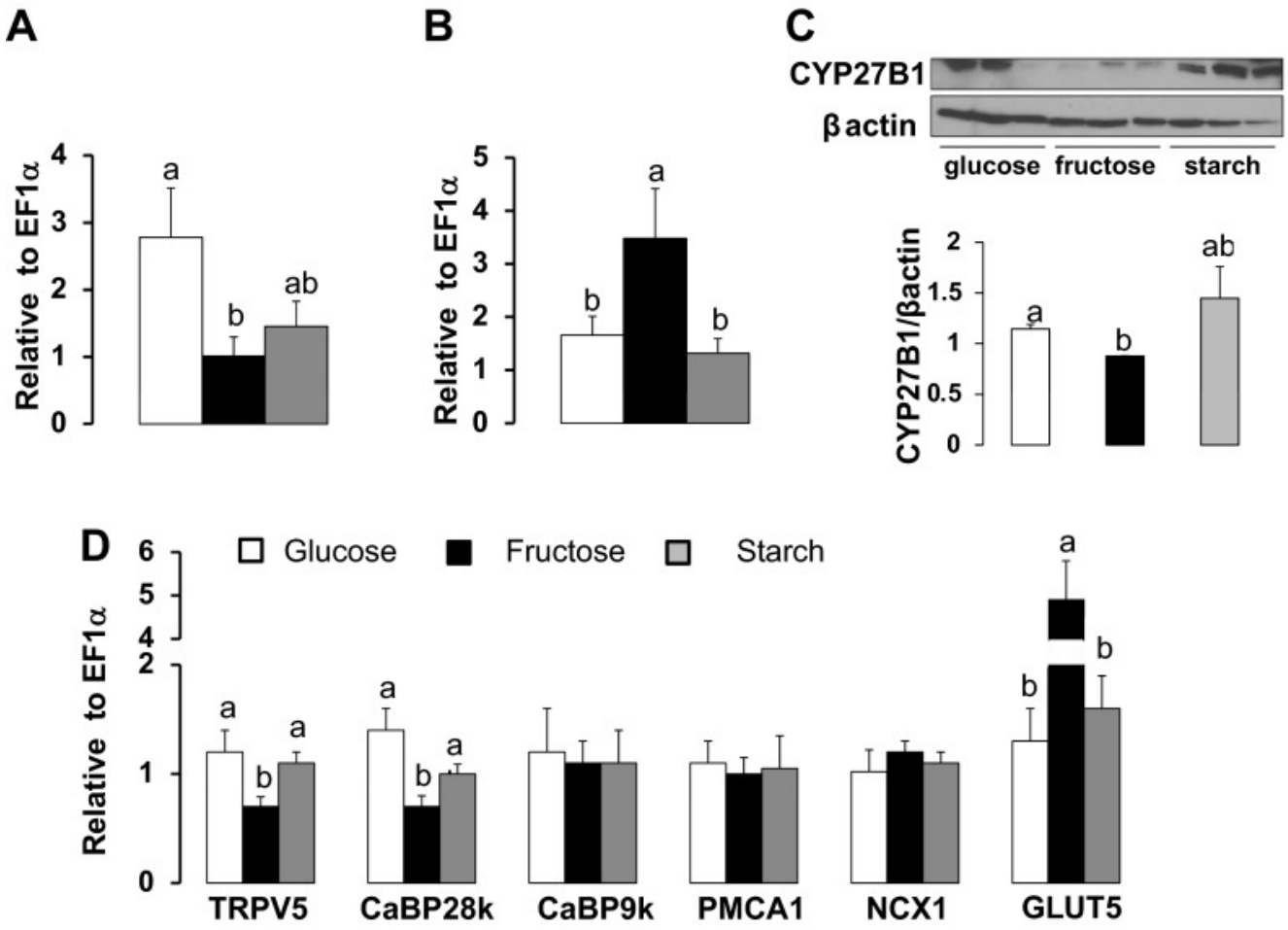

Open in a separate window

Expression of 1,25-$(OH)_2D_3$ metabolic enzymes and Ca^{2+} transporters in kidney of 50-day-old rats fed glucose, fructose, or starch after weaning. mRNA expression of CYP27B1 (*A*) and CYP24A1 (*B*) analyzed by real-time PCR using *EF1α* as a reference. *C*: protein abundance of CYP27B1 using β-actin as a reference. *D*: mRNA expression of TRPV5, CaBP28k, CaBP9k, PMCA1, NCX1, and GLUT5. All data were normalized relative to levels seen in rats fed starch. Data are means ± SE ($n = 8$ per group). Means with different superscript letters are significantly different at $P < 0.05$. CYP27B1, TRPV5, and CaBP28k mRNA expression each decreased with dietary fructose; CYP24A1 and GLUT5 expression increased with fructose.

Fig. 3.

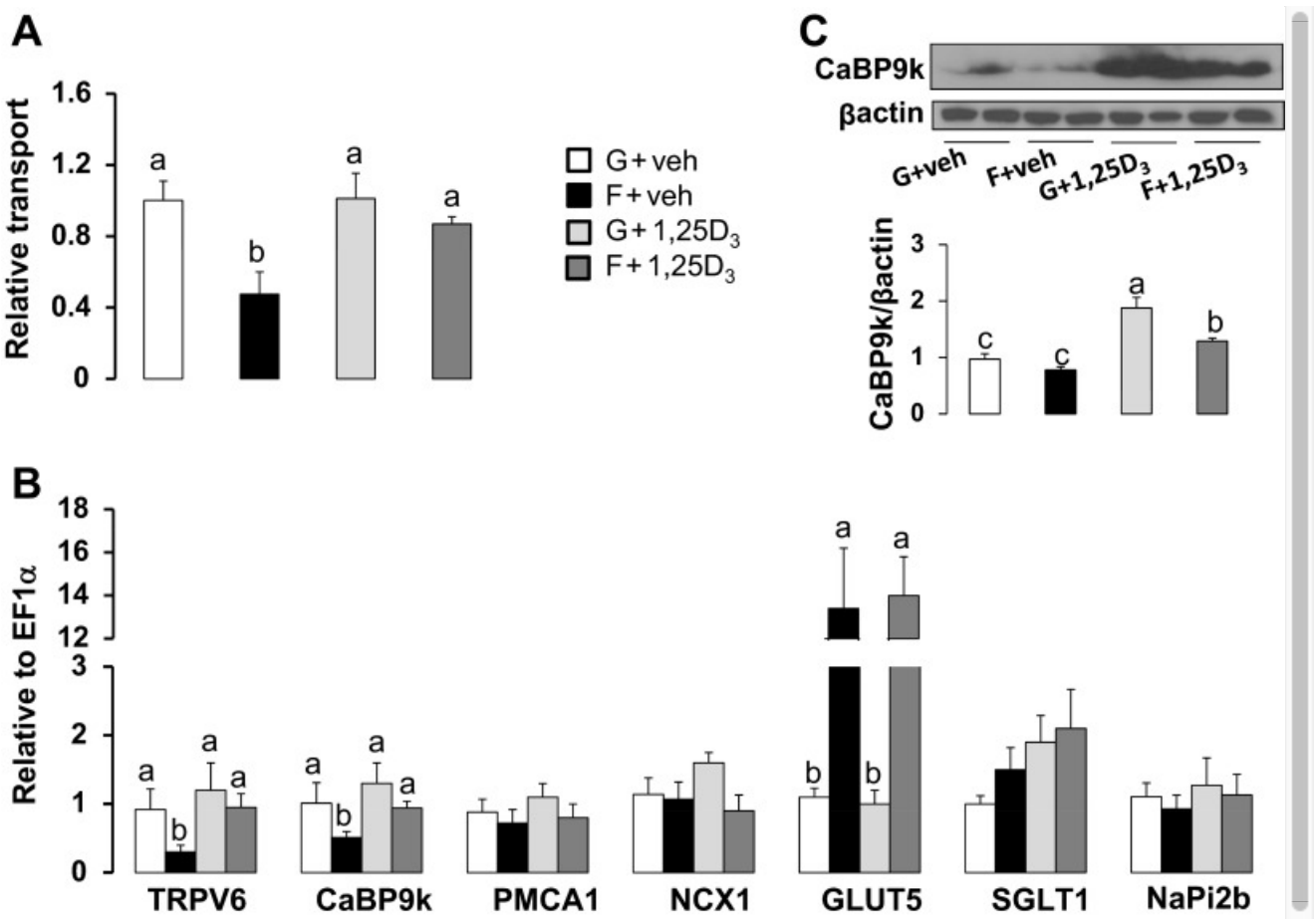

Open in a separate window

Treatment in vivo with 1,25-$(OH)_2D_3$ reverses fructose-dependent reductions in intestinal Ca^{2+} uptake and Ca^{2+} transporter expression. *A*: relative transepithelial Ca^{2+} transport from the luminal to the basolateral compartment expressed as a ratio of ($^{45}Ca_{inside}/^{45}Ca_{outside}$) of everted gut sacs. *B*: mRNA expression of Ca^{2+} (TRPV6, CaBP9k, PMCA1, NCX1), fructose (GLUT5), glucose (SGLT1), and phosphate (NaPi2b) transporters was analyzed by real-time PCR using *EF1α* as a reference. All data were normalized relative to levels seen in rats fed glucose and injected with vehicle. Data are means ± SE ($n = 6$ per group). Means with different superscript letters are significantly different ($P < 0.05$). Treatment with 1,25-$(OH)_2D_3$ prevented the fructose effect on the small intestine. *C*: protein abundance of CaBP9k using β-actin as a reference.

Fig. 4.

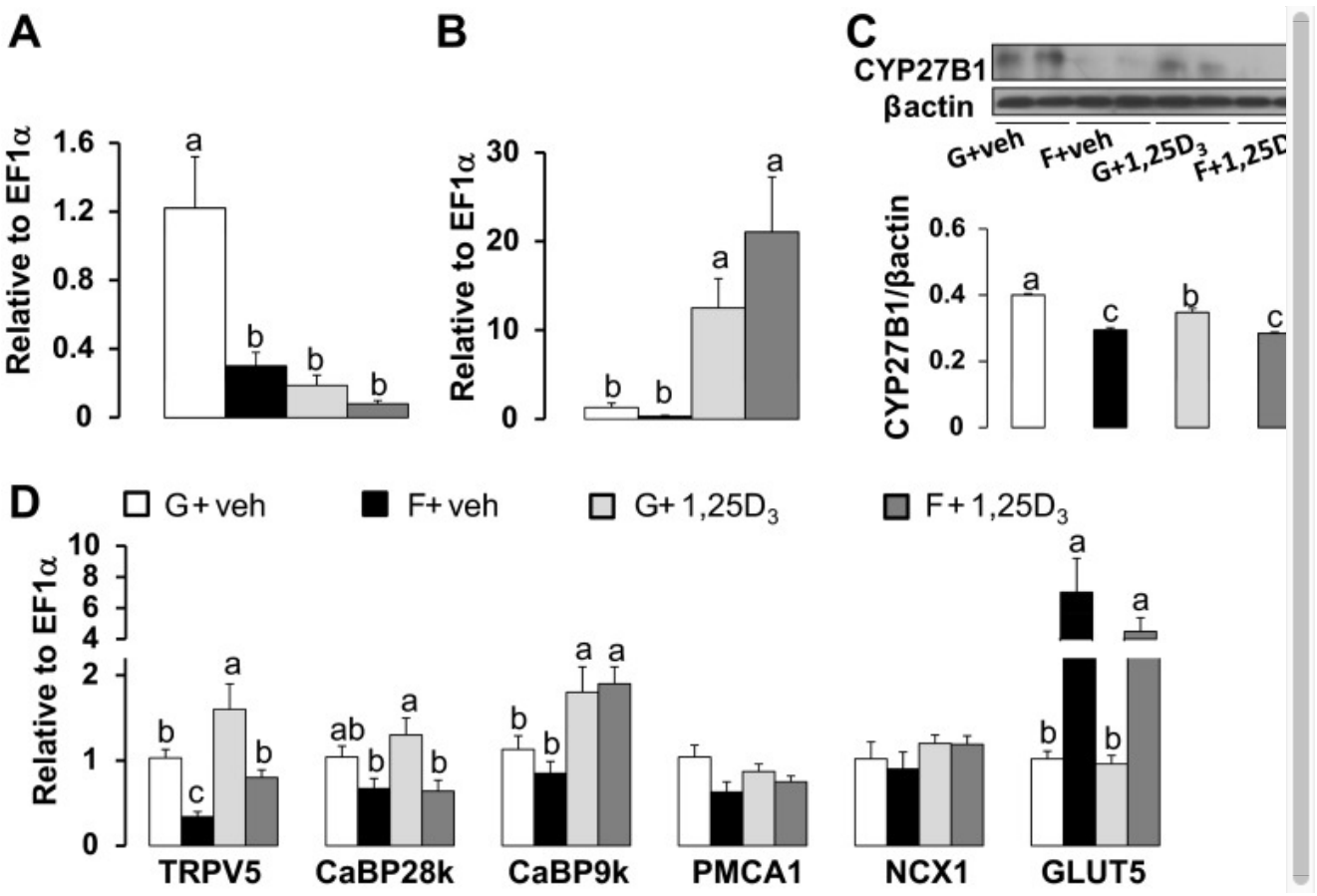

Open in a separate window

Effect of 1,25-$(OH)_2D_3$ treatment on renal expression of CYP27B1, CYP24A1, and Ca^{2+} transporters in postweaning rats fed glucose or fructose. mRNA expression of CYP27B1 (*A*), CYP24A1 (*B*), and protein abundance of CYP27B1 (*C*) using β-actin as a reference. *D*: TRPV5, CaBP28k, CaBP9k, PMCA1, NCX1, and GLUT5 were analyzed by real-time PCR using *EF1α* as a reference. All data were normalized relative to levels seen in rat fed glucose and injected with vehicle. Data are means ± SE ($n = 6$ per group). Means with different superscript letters are significantly different ($P < 0.05$). Treatment with 1,25-$(OH)_2D_3$ prevented the fructose effect on the kidney.

Table 2.

Serum biochemistry in 50-day-old rats fed glucose or fructose and then treated with 1,25-$(OH)_2$ D_3 or vehicle

	Vehicle		$1,25(OH)_2D_3$		Two-Way Significance		
	Glucose	Fructose	Glucose	Fructose	Diet	Rescue	Diet × Rescue
1,25-$(OH)_2D_3$, pmol/l	538 ± 78^a	357 ± 55^b	245 ± 65^b	261 ± 66^b	0.133	0.004	0.049
Calcium, mg/dl	10.1 ± 0.2^b	10.2 ± 0.2^b	11.4 ± 0.2^a	11.7 ± 0.3^a	0.523	0.0003	0.863

Open in a separate window

Data are means ± SE; $n = 6$ per group. Superscript letters refer to results of LSD post hoc tests after one-way ANOVA ($P < 0.05$). Means with different superscript letters are significantly different.

Fig. 5.

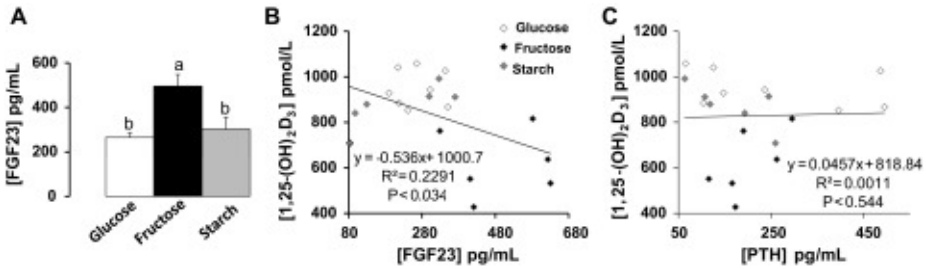

Open in a separate window

FGF23 and 1,25-$(OH)_2D_3$. *A*: circulating levels of FGF23 in rats fed glucose, fructose, or starch for 4 wk after weaning. *B*: variations in circulating levels of 1,25-$(OH)_2D_3$ are strongly negatively correlated with variations in circulating levels of FGF23. *C*: variations in circulating levels of 1,25-$(OH)_2D_3$ are independent of PTH levels. Means with different superscript letters are significantly different. 1,25-$(OH)_2D_3$ levels seem more strongly dependent on FGF23 but not PTH levels.

Fig. 6.

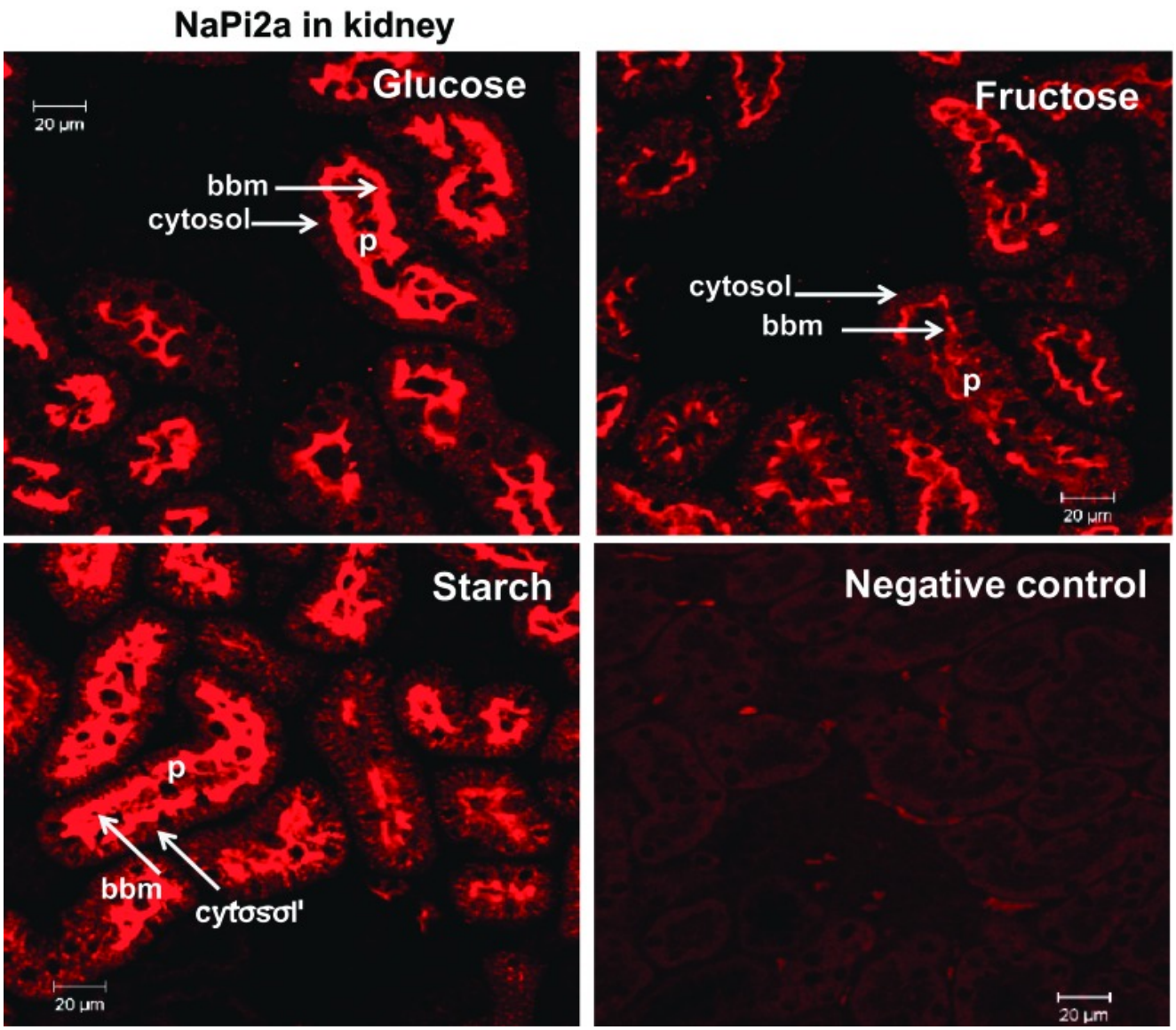

Open in a separate window

Effect of dietary fructose on NaPi2a expression in renal proximal tubules. Immunolocalization of FGF23-regulated Na^+-dependent phosphate transporter NaPi2a in renal proximal tubules (p) of 50-day-old rats fed glucose, fructose, or starch after weaning. Bars, 20 µm. White arrows indicate presence of NaPi2a in the apical or brushborder membrane (bbm) or its relatively low abundance in the cytosol of cells lining the proximal tubules. The negative control was processed without the primary antibody. Excessive fructose consumption clearly increased FGF23 to physiological levels high enough to reduce translocation of NaPi2a to the apical membrane of renal proximal tubule cells.

Fig. 7.

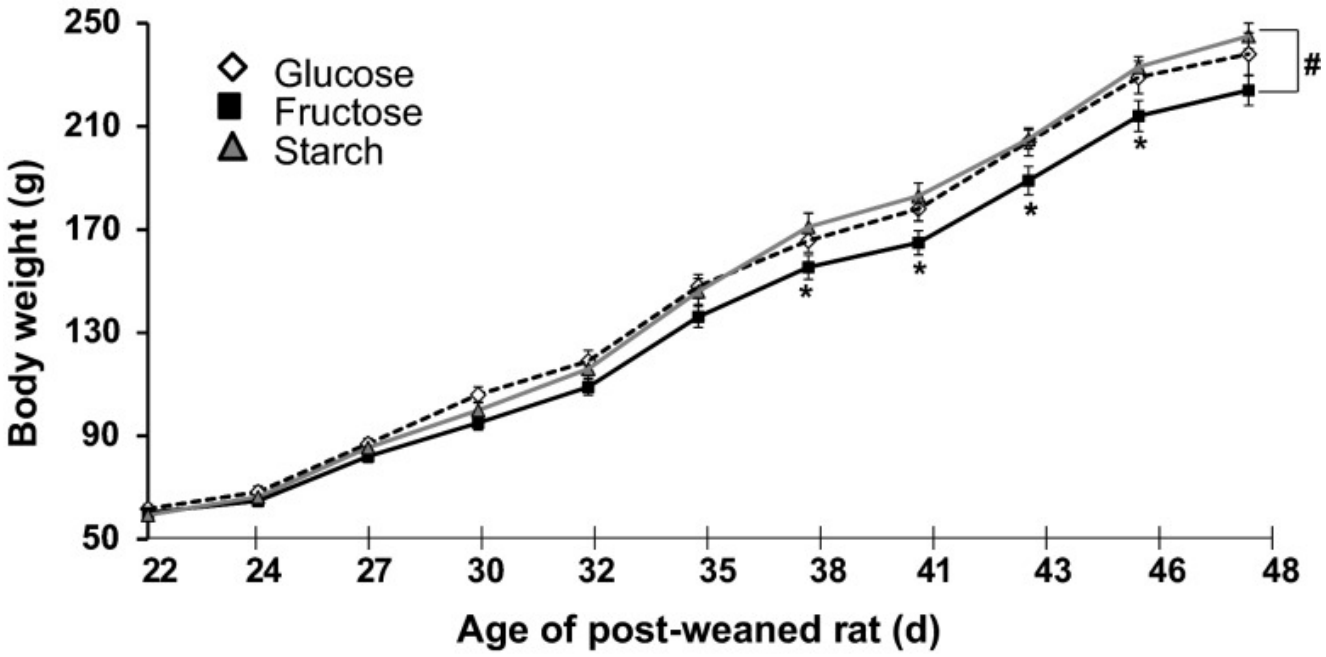

Body weight of weanling rats fed glucose, fructose, or starch diet for 4 wk. *Significant differences in body weight among the diets. Excessive intake of fructose gradually slowed the growth of rat pups.

Table 3.

Femora length and diameters

	Glucose	Fructose	Starch	Significance
Bone Length, mm	34.4 ± 0.6^{a}	32.4 ± 0.3^{b}	34.0 ± 0.6^{a}	0.031
Maximum outer diameter, a_o	4.33 ± 0.07	4.30 ± 0.12	4.46 ± 0.08	0.367
Minimum outer diameter, b_o	3.07 ± 0.09	2.95 ± 0.08	3.00 ± 0.05	0.469
Maximum inner diameter, a_i	3.23 ± 0.06	2.82 ± 0.14	2.70 ± 0.22	0.076
Minimum inner diameter, b_i	2.17 ± 0.07^{a}	1.85 ± 0.11^{b}	1.91 ± 0.12^{b}	0.028
Maximum cortical thickness, $a_o - a_i$	1.11 ± 0.05^{a}	1.48 ± 0.12^{b}	1.76 ± 0.17^{b}	0.018
Minimum cortical thickness, $b_o - b_i$	0.91 ± 0.09	1.10 ± 0.12	1.10 ± 0.10	0.241

Open in a separate window

Data are means ± SE in mm; $n = 6–8$ per group. Superscript letters refer to results of LSD post hoc tests after one-way ANOVA ($P < 0.05$). Means with different superscript letters are significantly different.

Table 4.

Humerus weight and mineral composition measurements

	Glucose	Fructose	Starch	Significance
Dry weight	206 ± 11^{a}	183 ± 8^{b}	201 ± 13^{a}	0.031
Total ash weight	126 ± 10^{a}	108 ± 6^{b}	120 ± 14^{a}	0.029
%Ash/bone	60.7 ± 2.0	59.2 ± 1.8	58.9 ± 2.8	0.874
Total weight of Ca^{2+}	45.0 ± 2.3	43.1 ± 1.7	47.9 ± 3.4	0.341
%Ca^{2+}/ash weight	34.6 ± 2.1	38.4 ± 0.9	37.0 ± 1.0	0.158
Total weight of P	25.7 ± 2.6^{a}	19.3 ± 0.4^{b}	22.2 ± 1.4^{ab}	0.023
%P/ash weight	19.8 ± 2.4	17.3 ± 0.4	17.2 ± 0.4	0.264
[Ca^{2+}] × [P]	1153 ± 114	837 ± 38	1089 ± 146	0.075

Open in a separate window

Data are means ± SE, weights in mg; $n = 6–8$ per group. Superscript letters refer to results of LSD post hoc tests after one-way ANOVA ($P < 0.05$). Means with different superscript letters are significantly different.

Fig. 8.

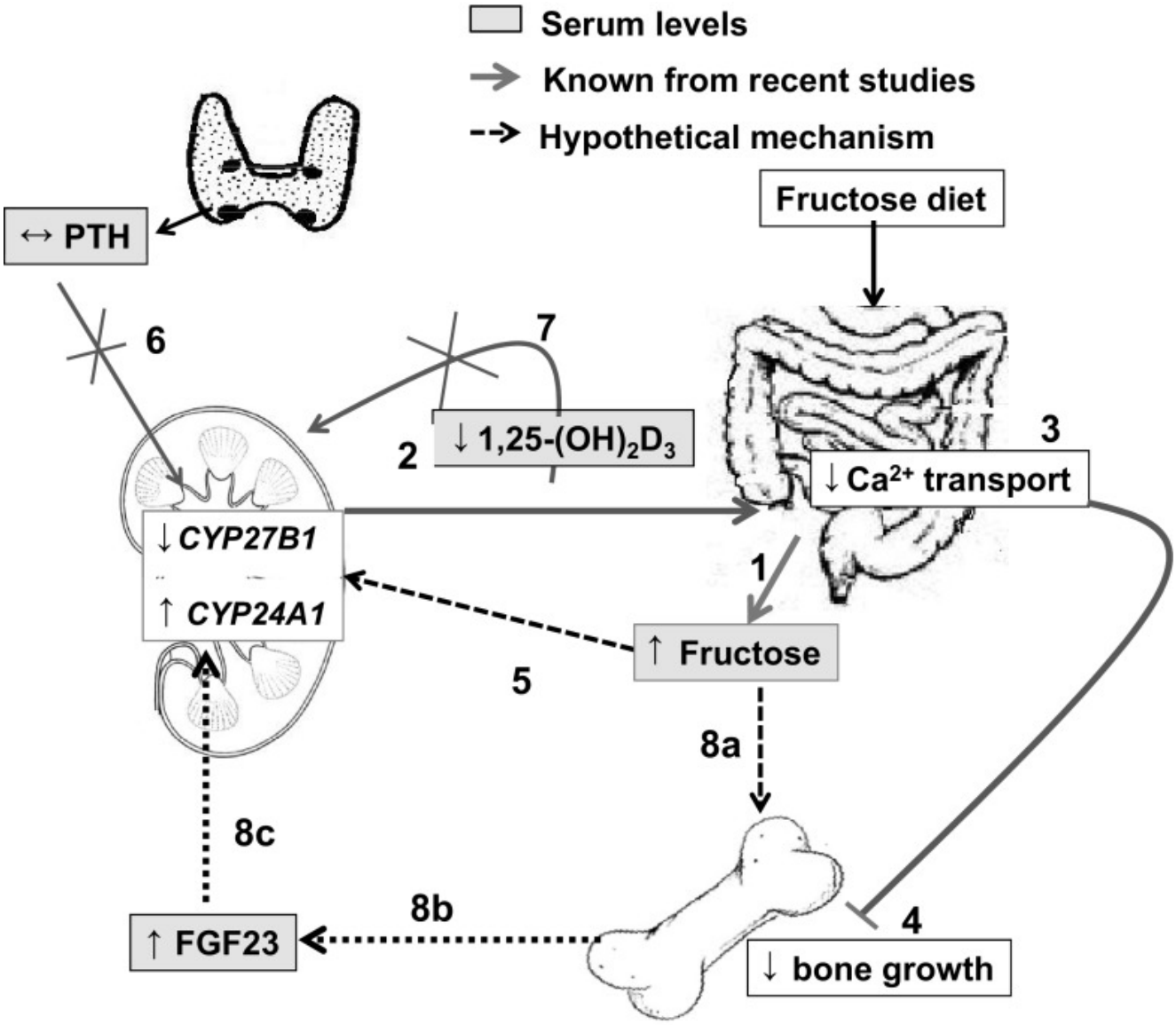

Open in a separate window

Schematic diagram of fructose-induced disruptions in 1,25-$(OH)_2D_3$ homeostasis. Under normal conditions such as in rats fed starch or glucose, postweaning growth stimulates increases in circulating levels of 1,25-$(OH)_2D_3$, which in turn enhance rates of intestinal Ca^{2+} transport, thereby addressing the increased Ca^{2+} demand for bone growth. Under fructose feeding, serum fructose increases (solid line with arrowhead, step 1). Fructose intake is associated with decrease in levels of 1,25-$(OH)_2D_3$ (*2*), resulting in reduced intestinal Ca^{2+} transport *(3)*, decreasing the supply of Ca^{2+} for appropriate growth (*4*; solid line with end point). Reduction in 1,25-$(OH)_2D_3$ levels results from increases in CYP24A1 and decreases in CYP27B1 renal expression, suggesting that fructose may directly enhance renal breakdown and impair synthesis of 1,25-$(OH)_2D_3$ (*5*, dashed arrow). These fructose effects were independent of any change in PTH (*6*) and the negative feedback loop by which 1,25-$(OH)_2D_3$ controls its own metabolism (*7*). Alternatively, fructose feeding is associated with an increase in circulating levels of FGF23, which may result from a direct effect of fructose on bone cells *(8a)*. This fructose-induced increase in FGF23 (*8b*) may be the mechanism by which fructose indirectly affects renal CYP27B1 and CYP24A1 expression (*8c*).